Aerospace Science and Technology 58 (2016) 178–188

Contents lists available at ScienceDirect

Aerospace Science and Technology

www.elsevier.com/locate/aescte

Free vibration of FG-CNT reinforced composite skew plates

Y. Kiani

Faculty of Engineering, Shahrekord University, Shahrekord, Iran

ARTICLE INFO

Article history:
Received 23 May 2016
Received in revised form 4 August 2016
Accepted 15 August 2016
Available online 22 August 2016

Keywords:
Carbon nanotube reinforced composite
Ritz method
Gram–Schmidt process
Skew plate
Functionally graded

ABSTRACT

Present study deals with the free vibration analysis of skew plates made from functionally graded carbon nanotube reinforced composites. Carbon nanotubes as reinforcements are distributed across the thickness of the plate. Distribution pattern may be uniform or functionally graded. The developed formulation from a Cartesian coordinate system is transformed to an oblique coordinate system to satisfy the boundary conditions. The virtual strain and kinetic energies of the plate are obtained using the first order shear deformation plate theory. Ritz method whose shape functions are developed according to the Gram–Schmidt process is implemented to construct an eigenvalue problem associated to the natural frequencies of the plate. The developed solution method is general and may be used for arbitrary boundary conditions of the plate. Results are compared for isotropic homogeneous and composite laminated plates in skew shape with the available data in the open literature. Afterwards numerical results are provided for skew plates reinforced with carbon nanotubes. It is shown that volume fraction of carbon nanotubes and their distribution pattern are both influential of natural frequencies of the carbon nanotube reinforced plates. Generally, the higher the volume fraction of carbon nanotubes, the higher the natural frequencies of the skew plate.

1. Introduction

Due to their exceptional mechanical properties, carbon nanotubes (CNTs) are known as an excellent candidate to reinforce the composites. CNTs have higher elasticity modulus in comparison to the polymeric and metallic matrices which results in a composite with enhanced stiffnesses. Therefore, volume fraction of CNTs is an important factor on structural response of composites reinforces with CNTs.

Another factor which may affect the global and local structural response of a composite media reinforced with CNTs is their distribution pattern. Distribution of CNTs in a matrix may be uniform or functionally graded according to a prescribed function. An overview of the available works on the mechanical and thermal properties of a composite media is provided by Liew et al. [1].

As shown by Shen [2], mechanical response of a rectangular plate may be enhanced with the introduction of a prescribed functionally graded pattern for the CNTs. Shen [2] exhibited that, bending moments of the plate may be alleviated significantly with the introduction of functionally graded CNTs where the top and bottom surfaces of the plate are enriched with the maximum volume fraction of CNT and the midsurface is free of CNT. Following this research, various investigators analysed the structural behaviour of CNT reinforced composites in various shapes. An overview of the available works on the vibration of plates made of functionally graded carbon nanotube reinforced composites (FG-CNTRC) is provided in the next paragraphs.

Based on the first order shear deformation plate theory and finite elements formulation, natural frequencies of an FG-CNTRC plate are obtained by Zhu et al. [3]. Free vibration of rectangular plates [4] and skew plates [5] are investigated by Zhang et al. using the element free methods. In two other studies, also, Zhang et al. [6,7] examined the free vibration characteristics of elastically restrained rectangular plates and plates which are simply supported in two opposite edges. For rectangular plates which are resting on elastic foundation, Zhang et al. [8] investigated the free vibration characteristics using an element free moving least squares Ritz formulation. For rectangular laminated plates with general boundary conditions and composed of FG-CNTRC layers, Lei et al. [9] investigated the free vibration characteristics using an element free method. Free vibration behaviour of FG-CNTRC plates in an arbitrary quadrilateral shape is investigated by Malekzadeh and Zarei [10] based on a two-dimensional generalised differential quadrature method. Malekzadeh and Heydarpour [11] developed a mixed solution method based on Navier and Layerwise formulations to investigate the free vibration characteristics of sandwich rectangular plates containing the FG-CNTRC layers. Due to the adoption of Navier solution method, plates which are simply supported all around may be analysed only. A higher order shear deformation

E-mail addresses: y.kiani@aut.ac.ir, y.kiani@eng.sku.ac.ir.

http://dx.doi.org/10.1016/j.ast.2016.08.018
1270-9638/

plate theory is used by Natarajan et al. [12] to investigate the free vibration of rectangular plates. Based on a two step perturbation technique, Wang and Shen [13,14] investigated the linear and nonlinear free vibration characteristics of FG-CNTRC plates and sandwich plates with FG-CNTRC face sheets. The provided solution method in these researches, may be used only for plates which are simply supported in flexure all around, while movable or immovable in normal to edges directions. Mirzaei and Kiani [15] applied the Chebyshev–Ritz method to the dynamic motion equations of the perforated plate to investigate the free vibration characteristics of moderately thick FG-CNTRC rectangular plate with a centric rectangular cut-out. Wang et al. [16] developed a semi-analytical solution to study the free vibration of thin rectangular FG-CNTRC plates using the classical plate theory formulation. Based on the conventional Ritz method accompanied with the Lagrangian multipliers technique, Kiani [17] investigated the free vibration characteristics of FG-CNTRC plates located on point supports. The solution method of this research is general and may be used for arbitrary number and position of point supports. Garcia-Macias et al. [18] analysed the free vibration and bending behaviour of FG-CNTRC skew plates. An efficient four-noded skew element with a total of twenty degrees of freedom is defined.

Similarly to free vibration behaviour of FG-CNTRC plates, forced vibration also has been the subject of many studies in the past years. However in comparison to free vibration, less attention is devoted to forced vibration. Dynamic response of rectangular plates made of FG-CNTRC plates subjected to dynamic loading is studied by Lei et al. [19] using a mesh free method. Wang and Shen [20] examined the geometrically nonlinear dynamic response of an FG-CNTRC rectangular plate under the action of lateral pressure. In this research, von-Kármán type of geometrical non-linearity is included into the formulation and plate is operating at various thermal environments. A two step perturbation technique suitable for plates with all edges simply supported is developed which may be used for both axially movable and immovable plates. Malekzadeh et al. [21] investigated the dynamic response of rectangular plate made of FG-CNTRC subjected to the action of a single moving mass. Finite element formulation is proposed to solve the motion equations of the plate suitable for arbitrary edge supports.

Above literature search reveals that, in comparison to rectangular plates, less attention is devoted to skew plates which is due to the more complex geometry. The present research examines the free vibration behaviour of moderately thick plates made of FG-CNTRC. First order shear deformation plate theory is used as the basic assumption to construct the kinetic and strain energies of the plate. The rectangular coordinate system is transformed to an oblique system which makes it easier to apply the boundary conditions of any type. Ritz minimization procedure is applied to the energies of the plate to establish the eigenvalue problem suitable for arbitrary in-plane and out-of-plane boundary conditions of the skew plate. To increase the convergence of the problem, the basis shape functions are approximated using the Gram–Schmidt orthogonal shape functions. The developed formulation is general and may be used for arbitrary combinations of boundary conditions. Numerical results of this study are compared with the available data in the open literature to assure the validity of the proposed formulation. Afterwards, parametric studies are given for FG-CNTRC skew plates.

2. Basic formulation

A skew plate with thickness h, edges a and b is considered. Orthogonal coordinate system is assigned to the corner of the mid-surface of the plate. The assigned coordinate system, geometrical characteristics and schematic of the plate are shown in Fig. 1.

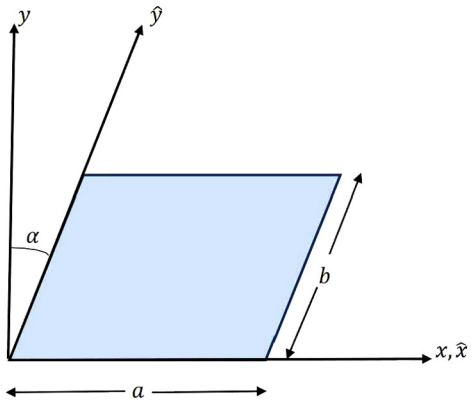

Fig. 1. Schematic, coordinate systems and geometrical characteristics of FG-CNTRC skew plate.

Table 1
Volume fraction of CNTs as a function of thickness coordinate for various cases of CNTs distribution [23–25].

CNTs distribution	V_{CN}
UD CNTRC	V^*_{CN}
FG-V CNTRC	$V^*_{CN}\left(1+2\frac{z}{h}\right)$
FG-O CNTRC	$2V^*_{CN}\left(1-2\frac{\lvert z\rvert}{h}\right)$
FG-X CNTRC	$4V^*_{CN}\frac{\lvert z\rvert}{h}$

Distribution of CNTs across the thickness of the plate may be uniform or functionally graded. When distribution of CNTs across the plate is functionally graded, it is usually referred to as functionally graded carbon nanotube reinforced composite (FG-CNTRC) skew plate. From the mathematical point of view, various dispersion profiles may be considered for the CNTs across the thickness of the plate, however, linearly graded patterns of CNTs are more observed in the researches due to their consistency with the fabrication processes [22]. As a result, three types of FG-CNTRC plates may be achieved which are known as FG-V, FG-X and FG-O. These three types along with the uniformly distributed (UD)-CNTRC skew plate are considered in the present research. Table 1 presents the distribution of volume fraction of CNT as a function of thickness coordinate in various CNTRC plates.

It is easy to check from Table 1 that, both uniform and functionally graded patterns of CNTRC plates will have the same total volume fraction of CNTs which is denoted by V^*_{CN}. Through such feature, the dynamic characteristics of UD- and FG-CNTRC may be compared with respect to each other. V^*_{CN} may be obtained as a function of mass density of CNTs, ρ^{CN}, mass density of matrix ρ^m and mass fraction of CNTs w^{CN} as

$$V^*_{CN} = \frac{w^{CN}}{w^{CN} + \rho^{CN}/\rho^m - w_{CN}\rho^{CN}/\rho^m} \tag{1}$$

Referring to Table 1 and comparing the distribution pattern of CNTs reveals that, in FG-X pattern, the top and bottom surfaces of the plate are enriched by the maximum volume fraction of CNTs whereas the mid-surface is free of CNTs. In FG-O, distribution pattern is inverse. The top and bottom surfaces are free of CNTs and the mid-surface is enriched with the maximum volume fraction of CNTs. In type FG-V, the bottom surface is free of CNT and the top one is enriched with the maximum volume fraction of CNT. In UD type, unlike the other four FG types, volume fraction of CNT is constant at each surface of the plate.

Various methods are proposed to estimate the effective material properties of the CNTRC media. Among them, Mori–Tanaka scheme

[26] and the rule of mixtures [27] approach are more observed through the researches. Rule of mixtures approach is a simple and efficient approach to obtain the properties of the fibre reinforced composite media. However, due to the severe differences between the properties of polymeric matrix and CNTs, this approach fails in accurate estimation of properties. A refined rule of mixtures which consists of efficiency parameters is used extensively in analysis of FG-CNTRC beams [28–33], plates [34], panels [35] and shells [24,25,36]. In the present study, also, this approach is used to estimate the overall mechanical properties of the composite media. In this approach auxiliary parameters are introduced into the rule of mixtures approach to match the data obtained by the rule of mixtures approach with those obtained by the molecular dynamics simulations [23]. Accordingly, Young's modulus and shear modulus of the composite media may be written as [23]

$$\begin{aligned} E_{11} &= \eta_1 V_{CN} E_{11}^{CN} + V_m E^m \\ \frac{\eta_2}{E_{22}} &= \frac{V_{CN}}{E_{22}^{CN}} + \frac{V_m}{E^m} \\ \frac{\eta_3}{G_{12}} &= \frac{V_{CN}}{G_{12}^{CN}} + \frac{V_m}{G^m} \end{aligned} \tag{2}$$

It is seen from Eq. (2) that, the refined rule of mixtures differs essentially from the conventional rule of mixtures approach in three efficiency parameters η_j, $j = 1, 2, 3$ which are used to capture the size dependent properties of the CNTRC plate. In Eq. (2), E_{11}^{CN}, E_{22}^{CN} and G_{12}^{CN} are the Young modulus and shear modulus of SWCNTs, respectively. Furthermore, E^m and G^m indicate the corresponding properties of the isotropic matrix. In Eq. (2) volume fraction of CNT and volume fraction of matrix are denoted by V_{CN} and V_m, respectively which should satisfy the condition

$$V_{CN} + V_m = 1 \tag{3}$$

As claimed by Shen [23], the effective Poisson ratio depends weakly on position and therefore takes the form

$$\nu_{12} = V_{CN}^{*} \nu_{12}^{CN} + V_m \nu^m \tag{4}$$

Conventional rule of mixtures is used generally to estimate the mass density of FG-CNTRC plates which dictates the dispersion profile of the mass density across the plate thickness as [13–15,24,29,35]

$$\rho = V_{CN} \rho^{CN} + V_m \rho^m \tag{5}$$

where as mentioned earlier, ρ^{CN} and ρ^m are the mass density of the CNT and matrix constituents, respectively. It is observed that, all types of FG-CNTRC and UD-CNTRC will have the same value of mass fraction of CNT.

In flexural theories, various estimations are proposed to conjecture the displacement components across the plate thickness. Some theories such as classical, first order and third order plate theories ignore the thickness stretching and some others take into account the thickness stretching [37–39]. However further considerations of these works reveal that, for functionally graded materials, divergence of natural frequencies based on first order shear deformation theory and these thickness stretchable theories is negligible. Therefore, in the present research, first order shear deformation plate theory is employed. It is known that, through usage of first order shear deformation plate theory, vibration characteristic of thin, moderately thick and even thick plates may be achieved accurately. According to the first order shear deformation plate theory, through the length, width and thickness displacement components of the plate may be written in terms of those belong to the mid-surface and cross section rotations as

$$\begin{aligned} u(x, y, z, t) &= u_0(x, y, t) + z\varphi_x(x, y, t) \\ v(x, y, z, t) &= v_0(x, y, t) + z\varphi_y(x, y, t) \\ w(x, y, z, t) &= w_0(x, y, t) \end{aligned} \tag{6}$$

Where in the above equation, displacement components u, v and w are associated to displacements along x, y and z directions, respectively. Besides, a subscript 0 indicates the characteristics of the mid-surface. Transverse normal rotations about the x and y axes are denoted by φ_y and φ_x are, respectively.

According to the first order theory, in-plane strain components are linear functions of thickness coordinate whereas out-of-plane shear strain components are constant across the thickness. Therefore one may write

$$\begin{Bmatrix} \varepsilon_{xx} \\ \varepsilon_{yy} \\ \gamma_{xy} \\ \gamma_{xz} \\ \gamma_{yz} \end{Bmatrix} = \begin{Bmatrix} \varepsilon_{xx0} \\ \varepsilon_{yy0} \\ \gamma_{xy0} \\ \gamma_{xz0} \\ \gamma_{yz0} \end{Bmatrix} + z \begin{Bmatrix} \kappa_{xx} \\ \kappa_{yy} \\ \kappa_{xy} \\ \kappa_{xz} \\ \kappa_{yz} \end{Bmatrix} \tag{7}$$

where, again the subscript 0 indicates the features of the mid-surface. The components of the strain on the mid-surface of the plate may be written as

$$\begin{Bmatrix} \varepsilon_{xx0} \\ \varepsilon_{yy0} \\ \gamma_{xy0} \\ \gamma_{xz0} \\ \gamma_{yz0} \end{Bmatrix} = \begin{Bmatrix} u_{0,x} \\ v_{0,y} \\ u_{0,y} + v_{0,x} \\ \varphi_x + w_{0,x} \\ \varphi_y + w_{0,y} \end{Bmatrix} \tag{8}$$

and the components of change in curvature compatible with the first order shear deformation theory are

$$\begin{Bmatrix} \kappa_{xx} \\ \kappa_{yy} \\ \kappa_{xy} \\ \kappa_{xz} \\ \kappa_{yz} \end{Bmatrix} = \begin{Bmatrix} \varphi_{x,x} \\ \varphi_{y,y} \\ \varphi_{x,y} + \varphi_{y,x} \\ 0 \\ 0 \end{Bmatrix} \tag{9}$$

where in the above equations and in the rest of this manuscript $()_{,x}$ and $()_{,y}$ denote the derivatives with respect to the x and y directions, respectively.

Under linear elastic deformations of the FG-CNTRC skew plates and compatible with the plane-stress conditions, constitutive law for the plate takes the form

$$\begin{Bmatrix} \sigma_{xx} \\ \sigma_{yy} \\ \tau_{yz} \\ \tau_{xz} \\ \tau_{xy} \end{Bmatrix} = \begin{bmatrix} Q_{11} & Q_{12} & 0 & 0 & 0 \\ Q_{12} & Q_{22} & 0 & 0 & 0 \\ 0 & 0 & Q_{44} & 0 & 0 \\ 0 & 0 & 0 & Q_{55} & 0 \\ 0 & 0 & 0 & 0 & Q_{66} \end{bmatrix} \begin{Bmatrix} \varepsilon_{xx} \\ \varepsilon_{yy} \\ \gamma_{yz} \\ \gamma_{xz} \\ \gamma_{xy} \end{Bmatrix} \tag{10}$$

where, in Eq. (10), Q_{ij} $(i, j = 1, 2, 4, 5, 6)$ are the reduced material stiffness coefficients compatible with the plane-stress conditions and are obtained in terms of the elasticity and shear modulus as well as the Poisson ratios as [24]

$$\begin{aligned} &Q_{11} = \frac{E_{11}}{1 - \nu_{12}\nu_{21}}, \quad Q_{22} = \frac{E_{22}}{1 - \nu_{12}\nu_{21}}, \quad Q_{12} = \frac{\nu_{21} E_{11}}{1 - \nu_{12}\nu_{21}} \\ &Q_{44} = G_{23}, \quad Q_{55} = G_{13}, \quad Q_{66} = G_{12} \end{aligned} \tag{11}$$

In order to satisfy the boundary conditions on the plate it is more appropriate to use the oblique coordinate system $(\overline{x}, \overline{y})$ instead of the previously defined orthogonal coordinate system (x, y). From simply geometry the oblique coordinate is given by

$$\overline{x} = x - y\tan(\alpha)$$
$$\overline{y} = y\sec(\alpha) \tag{12}$$

The components of rotations in the oblique coordinates are obtained as

$$\varphi_x(x,y,t) = \varphi_{\overline{x}}(\overline{x},\overline{y},t)\cos(\alpha)$$
$$\varphi_y(x,y,t) = -\varphi_{\overline{x}}(\overline{x},\overline{y},t)\sin(\alpha) + \varphi_{\overline{y}}(\overline{x},\overline{y},t) \tag{13}$$

And the partial derivatives are related by

$$()_{,x} = ()_{,\overline{x}}$$
$$()_{,y} = -()_{,\overline{x}}\tan(\alpha) + ()_{,\overline{y}}\sec(\alpha) \tag{14}$$

In the oblique coordinate system the components of the mid-surface strain field from Eq. (8) change to

$$\begin{Bmatrix} \varepsilon_{xx0} \\ \varepsilon_{yy0} \\ \gamma_{xy0} \\ \gamma_{xz0} \\ \gamma_{yz0} \end{Bmatrix} = \begin{Bmatrix} u_{0,\overline{x}} \\ v_{0,\overline{y}}\sec(\alpha) - v_{0,\overline{x}}\tan(\alpha) \\ u_{0,\overline{y}}\sec(\alpha) - u_{0,\overline{x}}\tan(\alpha) + v_{0,\overline{x}} \\ \varphi_{\overline{x}}\cos(\alpha) + w_{0,\overline{x}} \\ \varphi_{\overline{y}} - \varphi_{\overline{x}}\sin(\alpha) + w_{0,\overline{y}}\sec(\alpha) - w_{0,\overline{x}}\tan(\alpha) \end{Bmatrix} \tag{15}$$

And the components of change of curvature from Eq. (9) with the aid of Eqs. (13) and (14) change to

$$\begin{Bmatrix} \kappa_{xx} \\ \kappa_{yy} \\ \kappa_{xy} \\ \kappa_{xz} \\ \kappa_{yz} \end{Bmatrix} = \begin{Bmatrix} \varphi_{\overline{x},\overline{x}}\cos(\alpha) \\ \varphi_{\overline{y},\overline{y}}\sec(\alpha) + \varphi_{\overline{x},\overline{x}}\sec(\alpha)\tan(\alpha) - \varphi_{\overline{x},\overline{y}}\tan(\alpha) - \varphi_{\overline{y},\overline{x}}\tan(\alpha) \\ \varphi_{\overline{x},\overline{y}} + \varphi_{\overline{y},\overline{x}} - 2\varphi_{\overline{x},\overline{x}}\sin(\alpha) \\ 0 \\ 0 \end{Bmatrix} \tag{16}$$

To obtain the motion equations of the skew plate, Hamilton's principle may be used [40]. For the case of freely vibrating skew plate when external forces are absent, Hamilton's principle takes the form [40]

$$\int_{t_1}^{t_2} \delta(U - T)dt = 0$$
$$t = t_1, t_2 : \delta u_0 = \delta v_0 = \delta w_0 = \delta\varphi_{\overline{x}} = \delta\varphi_{\overline{y}} = 0 \tag{17}$$

where in Eq. (17), δU is the virtual strain energy of the skew plate in the oblique coordinate system which may be calculated as

$$\delta U = \int_0^a \int_0^b \int_{-0.5h}^{+0.5h} (\sigma_{xx}\delta\varepsilon_{xx} + \sigma_{yy}\delta\varepsilon_{yy} + \tau_{xy}\delta\gamma_{xy} + \kappa\tau_{xz}\delta\gamma_{xz} + \kappa\tau_{yz}\delta\gamma_{yz})dzd\overline{y}d\overline{x} \tag{18}$$

In the above equations, κ is the shear correction factor. Evaluation of the exact value of this factor is not straightforward since it depends on geometric characteristics, boundary conditions, material type and loading conditions. Meanwhile through the open literature, the approximate values of $\kappa = 1$, $\kappa = 5/6$ and $\kappa = \pi^2/12$ are used extensively even for composites and FGMs. In this research, κ is set equal to $\kappa = 5/(6 - \nu_{12}^{CN}V_m - \nu^m V_{CN})$ which is used extensively by Liew and his co-authors in structural examination of FG-CNTRC beams, plates and shells [4,5].

Similarly, δT is the variation of kinetic energy of the skew plate which also may be written as

$$\delta T = \int_0^a \int_0^b \int_{-0.5h}^{+0.5h} \rho(z)\,(\dot{u}\delta\dot{u} + \dot{v}\delta\dot{v} + \dot{w}\delta\dot{w})\,dzd\overline{y}d\overline{x} \tag{19}$$

3. Space approximation

Recalling Eqs. (18) and (19) and applying the Green–Gauss theorem to the Hamilton Equation (17) may result in the five coupled partial differential equations and the associated boundary conditions. On the other hand, energy based techniques also may be used to solve the problem. Conventional Ritz method as a powerful tool is used in this study to obtain the matrix representation of the governing equations associated to the motion equations of a skew plate under free vibration regime. Beforehand, using the general idea of separation of variables technique, each of the essential variables of the problem, i.e. u_0, v_0, w_0, $\varphi_{\overline{x}}$ and $\varphi_{\overline{y}}$ may be written as

$$u_0(\overline{x},\overline{y},t) = \sum_{i=0}^{N_x}\sum_{j=0}^{N_y} U_{ij}(t)N_i^u(\overline{x})N_j^u(\overline{y})$$
$$v_0(\overline{x},\overline{y},t) = \sum_{i=0}^{N_x}\sum_{j=0}^{N_y} V_{ij}(t)N_i^v(\overline{x})N_j^v(\overline{y})$$
$$w_0(\overline{x},\overline{y},t) = \sum_{i=0}^{N_x}\sum_{j=0}^{N_y} W_{ij}(t)N_i^w(\overline{x})N_j^w(\overline{y})$$
$$\varphi_x(\overline{x},\overline{y},t) = \sum_{i=0}^{N_x}\sum_{j=0}^{N_y} X_{ij}(t)N_i^x(\overline{x})N_j^x(\overline{y})$$
$$\varphi_y(\overline{x},\overline{y},t) = \sum_{i=0}^{N_x}\sum_{j=0}^{N_y} Y_{ij}(t)N_i^y(\overline{x})N_j^y(\overline{y}) \tag{20}$$

where in the above equations $N_i^\alpha(\overline{x})$, $i = 0,1,2,...,N_x$, $N_j^\alpha(\overline{y})$, $j = 0,1,2,...,N_y$, $\alpha = u, v, w, x, y$ are the shape functions which have to be chosen according to the essential boundary conditions. Various types of shape functions are used extensively by researchers. Polynomial shape functions, trigonometric and those developed based on Chebyshev polynomials are used extensively. Also another type of shape functions which are of interest in the open literature are those developed using the Gram–Schmidt process. This process develops a set of orthogonal shape functions of various type. In the rest an overview of this process is provided.

4. Gram–Schmidt process

Given a function (polynomial) $\xi_0(s)$, an orthogonal set of functions (polynomials) may be developed in an arbitrary interval $c \le s \le d$ according to Gram–Schmidt process as follows

$$\xi_1(s) = (s - \zeta_1)\xi_0(s)$$
$$\xi_k(s) = (s - \zeta_k)\xi_{k-1}(s) - \eta_k\xi_{k-2}(s), \qquad k \ge 2 \tag{21}$$

where in the above equation, ζ_k and η_k are obtained as

$$\zeta_k = \frac{\int_c^d sq(s)\xi_{k-1}^2(s)ds}{\int_c^d q(s)\xi_{k-1}^2(s)ds}, \qquad k \ge 1$$
$$\eta_k = \frac{\int_c^d sq(s)\xi_{k-1}(s)\xi_{k-2}(s)ds}{\int_c^d q(s)\xi_{k-2}^2(s)ds}, \qquad k \ge 2 \tag{22}$$

where in the above equations $q(s)$ is the weight function. It is easy to check that, the developed set of functions $\xi_k(s), k = 0,1,2,...$ according to the above process are orthogonal with respect to the weight function $q(s)$ in the interval $c \le s \le d$. Equivalently the following property is established between the functions $\xi_k(s), k = 0,1,2,...$

Table 2
Convergence study on the first six flexural frequency parameters $\widehat{\omega} = \omega b^2\sqrt{\rho h/D}/\pi^2$ of CCCC skew plates with $a/h = 1000$, $a/b = 1$, $\alpha = 45^\circ$ and $\nu = 0.3$. D is the flexural rigidity.

$N_x = N_y$	$\widehat{\omega}_1$	$\widehat{\omega}_2$	$\widehat{\omega}_3$	$\widehat{\omega}_4$	$\widehat{\omega}_5$	$\widehat{\omega}_6$
4	7.1296	13.3617	19.0393	25.6579	1453.4504	1751.6810
6	6.6786	10.9260	16.1079	16.4327	24.7142	26.7992
8	6.6589	10.7968	15.0619	15.9948	20.2323	23.5748
10	6.6548	10.7956	15.0389	15.9504	19.9588	23.2818
12	6.6530	10.7936	15.0341	15.9410	19.9462	23.2647
14	6.6507	10.7901	15.0297	15.9343	19.9390	23.2568
Liew et al. [44]	6.6519	10.7898	15.0476	15.9342	19.9365	23.2526

Table 3
First six flexural natural frequency parameters $\widehat{\omega} = \omega b^2\sqrt{\rho h/D}/\pi^2$ of skew plates with $a/h = 1000$, $a/b = 1$, $\alpha = 30^\circ$ and $\nu = 0.3$. D is the flexural rigidity.

B.Cs.	Source	$\widehat{\omega}_1$	$\widehat{\omega}_2$	$\widehat{\omega}_3$	$\widehat{\omega}_4$	$\widehat{\omega}_5$	$\widehat{\omega}_6$
CCCC	Present	4.6697	8.2677	10.6570	12.0860	16.7207	16.7545
	Liew et al. [44]	4.6698	8.2677	10.6554	12.0825	16.7159	16.7496
SSSS	Present	2.5310	5.3338	7.2858	8.4982	12.4454	12.4454
	Liew et al. [44]	2.5294	5.3333	7.2821	8.4966	12.4442	12.4442
SCSC	Present	3.7446	6.5118	9.4222	10.2125	13.9538	14.4610
	Liew et al. [44]	3.7451	6.5119	9.4233	10.2112	13.9530	14.4581
FSFS	Present	1.2310	1.7944	3.6500	5.0062	6.2131	6.6440
	Liew et al. [44]	1.2310	1.7948	3.6504	5.0063	6.2150	6.6446
FCFC	Present	2.7761	3.0955	5.0139	7.4904	8.2025	8.6340
	Liew et al. [44]	2.7763	3.0952	5.0154	7.4898	8.2003	8.6350
CFFF	Present	0.3982	0.9537	2.5629	2.6274	4.1881	5.1296
	Liew et al. [44]	0.3983	0.9537	2.5631	2.6277	4.1887	5.1309

Table 4
First six flexural frequency parameter $\widehat{\omega} = \omega a^2/h\sqrt{\rho/E_{22}}/\pi^2$ of [90/0/90/0/90] SSSS composite laminated skew plate with various skew angles. Side to thickness ratio is $a/h = 1000$ and aspect ratio is $a/b = 1$. Material properties are $E_{11}/E_{22} = 40$, $G_{12}/E_{22} = G_{13}/E_{22} = 0.6$, $G_{23}/E_{22} = 0.5$ and $\nu_{12} = 0.25$.

$\widehat{\omega}_1$	$\alpha = 0$		$\alpha = 30^\circ$		$\alpha = 45^\circ$	
	Present	Wang [45]	Present	Wang [45]	Present	Wang [45]
$\widehat{\omega}_1$	1.9140	1.9141	2.8286	2.8248	4.4919	4.4786
$\widehat{\omega}_2$	3.9744	3.9745	5.1917	5.1891	7.1174	7.1121
$\widehat{\omega}_3$	6.6559	6.6567	8.4828	8.4836	10.4496	10.4512
$\widehat{\omega}_4$	7.6559	7.6564	9.2616	9.2574	14.0985	14.1024
$\widehat{\omega}_5$	8.1504	8.1511	12.1151	12.1070	14.7980	14.7797
$\widehat{\omega}_6$	10.6237	10.6249	12.1295	12.1301	17.9521	17.9628

$$\int_c^d q(s)\xi_n(s)\xi_m(s)ds = a_{mn} \tag{23}$$

where a_{mn} is nonzero when m and n are identical. Otherwise, a_{mn} is equal to zero.

5. Fundamental shape function

The process mentioned in the previous section may be used to generate the shape functions in both $\overline{x}$ and $\overline{y}$ directions for each of the essential variables $u_0, v_0, w_0, \varphi_{\overline{x}}$ and $\varphi_{\overline{y}}$. In the present research the weight function is chosen as $q(\overline{x}) = q(\overline{y}) = 1$ and the problem domain is $0 \le \overline{x} \le a$ and $0 \le \overline{y} \le b$. As seen from the recursive Eq. (21), the complete set of orthogonal shape functions depends of the choice of the first one, $\xi_0(s)$. This function should be chosen according to the essential boundary conditions of the problem. For a skew plate, three types of boundary conditions are used extensively. A clamped (C) edge in which both of the rotations and three components of the displacements are equal to zero at the edge. A free edge (F) where none of the rotations and displacements are equal to zero at the edge. And finally a simply supported (S) one, in which lateral and tangential displacement and the tangential slope are restrained at the support. As an example of choosing the fundamental shape function for each of the essential variables consider a plate which is simply supported at $x = 0$, clamped at $x = a$, free at $y = b$ and simply supported at $y = 0$. Therefore the fundamental shape functions for such plate may be considered as

$$\begin{aligned}
N_0^u(\overline{x}) &= 1 - \frac{\overline{x}}{a}, & N_0^u(\overline{y}) &= \frac{\overline{y}}{b}\\
N_0^v(\overline{x}) &= \frac{\overline{x}}{a}\left(1 - \frac{\overline{x}}{a}\right), & N_0^v(\overline{y}) &= 1\\
N_0^w(\overline{x}) &= \frac{\overline{x}}{a}\left(1 - \frac{\overline{x}}{a}\right), & N_0^w(\overline{y}) &= \frac{\overline{y}}{b}\\
N_0^x(\overline{x}) &= 1 - \frac{\overline{x}}{a}, & N_0^x(\overline{y}) &= \frac{\overline{y}}{b}\\
N_0^y(\overline{x}) &= \frac{\overline{x}}{a}\left(1 - \frac{\overline{x}}{a}\right), & N_0^y(\overline{y}) &= 1
\end{aligned} \tag{24}$$

With the introduction of the above functions and the simultaneous aid of Eqs. (21) and (22), the complete set of orthogonal shape functions may be achieved. Afterwards the motion equations describing the dynamic response of a skew plate under free vibration motion takes the form

$$\mathbf{M}\ddot{\mathbf{X}} + \mathbf{K}\mathbf{X} = 0 \tag{25}$$

where as usual $\mathbf{M}$ is the mass matrix and $\mathbf{K}$ is the stiffness matrix. Besides, $\mathbf{X}$ is the unknown displacement vector comprising the unknowns $U_{ij}, V_{ij}, W_{ij}, X_{ij}$ and Y_{ij} where $i = 0, 1, 2, \ldots N_x$ and $j = 0, 1, 2, \ldots, N_y$. For a freely vibrating skew plate, $\mathbf{X} = \widehat{\mathbf{X}}\sin(\omega t + \alpha)$ where ω is the natural frequency. Consequently, Eq. (25) alters to

$$\left(\mathbf{K} - \omega^2\mathbf{M}\right)\widehat{\mathbf{X}} = 0 \tag{26}$$

The above equation should be treated as a standard eigenvalue problem to obtain the frequencies.

Table 5
First six natural frequency parameters $\widehat{\omega} = \omega b^2\sqrt{\rho_m h/D_m}/\pi^2$ for skew plates with CCCC boundary conditions. Geometrical characteristics of the plate are $a/b = 1$ and $b/h = 20$.

α	V^*_{CN}	Type	$\widehat{\omega}_1$	$\widehat{\omega}_2$	$\widehat{\omega}_3$	$\widehat{\omega}_4$	$\widehat{\omega}_5$	$\widehat{\omega}_6$
30°	0.12	UD	9.0583	11.7968	16.8446	18.4411	20.7125	22.5152
		FG-X	9.6602	12.4074	17.5573	19.2855	21.5554	23.3963
		FG-O	7.9610	10.8772	15.9129	16.8411	19.3541	21.2748
		FG-V	8.4951	11.4120	16.5463	17.6404	20.1338	22.0743
	0.17	UD	11.4123	15.0207	21.5717	23.4079	26.4269	28.8189
		FG-X	12.3012	16.0088	22.8119	24.6875	27.7964	30.3308
		FG-O	9.9266	13.7295	20.1952	21.2054	24.5179	27.0092
		FG-V	10.6672	14.5466	21.2215	22.3422	25.7146	28.2752
	0.28	UD	12.6627	16.2668	23.0436	25.5011	28.4573	30.8028
		FG-X	13.7830	17.8621	25.3503	27.2345	30.6717	33.5410
		FG-O	11.2550	14.8361	21.3919	23.7192	26.6464	28.8476
		FG-V	12.1026	16.0115	23.0154	24.9197	28.2274	30.6832
45°	0.12	UD	10.2574	14.6655	20.6211	20.6301	25.7779	26.5480
		FG-X	10.8706	15.3507	21.4855	21.4925	26.6815	27.5437
		FG-O	9.2285	13.6982	19.1727	19.3654	24.6218	25.0891
		FG-V	9.7632	14.2984	19.9719	20.1377	25.4415	25.9911
	0.17	UD	12.9865	18.7299	26.2869	26.3612	33.0683	33.9720
		FG-X	13.9237	19.8764	27.6600	27.8182	34.6762	35.6684
		FG-O	11.5794	17.3423	24.2539	24.5488	31.3546	31.8628
		FG-V	12.3501	18.2796	25.4515	25.7399	32.7181	33.2505
	0.28	UD	14.2484	20.1398	28.2663	28.3871	35.1731	36.3295
		FG-X	15.5727	22.1298	30.5102	30.8215	38.2574	39.3400
		FG-O	12.8198	18.5517	26.3314	26.5460	33.1899	34.1695
		FG-V	13.8087	19.9432	27.9644	28.0509	35.3815	35.9552
60°	0.12	UD	14.3441	21.2986	28.0159	29.1989	34.8581	38.5037
		FG-X	15.0132	22.1782	29.0559	30.1434	35.9802	39.6530
		FG-O	13.4143	20.0716	26.4956	28.0687	33.1799	37.1003
		FG-V	13.9850	20.8122	27.3636	28.9034	34.1054	38.0633
	0.17	UD	18.3160	27.2434	35.8500	37.4982	44.6560	49.4709
		FG-X	19.4256	28.7330	37.6159	39.2064	46.5953	51.5734
		FG-O	16.9959	25.4765	33.6661	35.8098	42.2355	47.3648
		FG-V	17.8807	26.5760	34.8634	37.1915	43.4171	48.7724
	0.28	UD	19.7023	29.1797	38.3444	39.7714	47.6200	52.4028
		FG-X	21.6149	31.8309	41.4634	43.1621	51.1081	56.6188
		FG-O	18.1597	27.2138	36.1059	37.7446	45.3288	50.0296
		FG-V	19.4751	28.4503	34.6722	34.6941	36.8723	39.7587

6. Numerical results and discussion

The procedure outline in the previous sections in used to study the free vibration response of FG-CNTRC skew plates. The developed solution method is general and may be used for arbitrary types of in-plane and out-of-plane boundary conditions.

In the rest of this manuscript, the following convention is established for boundary conditions. For instance, an SCFC skew plate, indicates a plate which is simply supported at $x = 0$, clamped at $y = 0$, clamped at $y = b$, and free at $x = a$. Unless otherwise stated, Poly (methyl methacrylate), referred to as PMMA, is selected for the matrix with material properties $E^m = 2.5$ GPa, $\nu^m = 0.34$ and $\rho^m = 1150$ kg/m^3. (10,10) armchair SWCNT (tube length 9.26 nm, tube radius 0.68 nm and tube thickness = 0.067 nm) is chosen as the reinforcements. Elasticity modulus, shear modulus, Poisson's ratio and mass density of SWCNT are evaluated at reference temperature by Shen and Xiang [41] and are $E^{CN}_{11} = 5.6466$ TPa, $E^{CN}_{22} = 7.0800$ TPa, $G_{12} = 1.9445$ TPa, $\nu = 0.175$ and $\rho = 1400$ kg/m^3.

Han and Elliott [42] performed a molecular dynamics simulation to obtain the mechanical properties of nanocomposites reinforced with SWCNT. However in their analysis the effective thickness of CNT is assumed to be at least 0.34 nm. The thickness of CNT as reported should be at most 0.142 nm [43]. Therefore molecular dynamics simulation of Han and Elliott [42] is re-examined [23]. The so-called efficiency parameters, as stated earlier, are chosen to match the data obtained by the modified rule of mixtures of the present study and the re-examined molecular dynamics simulation results. For three different volume fractions of CNTs, these parameters are as: $\eta_1 = 0.137$ and $\eta_2 = 1.022$ for $V^*_{CN} = 0.12$. $\eta_1 = 0.142$ and $\eta_2 = 1.626$ for $V^*_{CN} = 0.17$. $\eta_1 = 0.141$ and $\eta_2 = 1.585$ for $V^*_{CN} = 0.28$. For each case, the efficiency parameter η_3 is equal to $0.7\eta_2$. The shear modulus G_{13} is taken equal to G_{12} whereas G_{23} is taken equal to $1.2G_{12}$ [23].

6.1. Convergence and comparison studies

In this section, convergence and comparison studies are provided. At first a convergence study is given for the natural frequencies of a completely clamped isotropic homogeneous skew plate. Dimensions of the plate for the sake of comparison are $a/b = 1$, $a/h = 1000$ and $\alpha = 45°$. Results of this study are obtained according to the present Ritz formulation for various number of shape functions and compared with those obtained by Liew et al. [44] which are obtained according to the first order shear deformation plate theory. Comparison is provided in Table 2. It is seen that, the first six frequency parameters are converged and are in excellent agreement with those of Liew et al. [44] after adoption of 14 shape functions in each direction of the plate for each of the essential variables. Therefore, in the subsequent results the number of shape functions is chosen as $N_x = N_y = 14$.

The next comparison study, provided in Table 3 compares the first six frequency parameters of skew plates made of an isotropic

Table 6
First six natural frequency parameters $\widehat{\omega} = \omega b^2\sqrt{\rho_m h/D_m}/\pi^2$ for skew plates with $V^*_{CN} = 0.17$, $\alpha = 45^\circ$ and various boundary conditions. Geometrical characteristics of the plate are $a/b = 1$ and $b/h = 20$.

B.Cs.	Type	$\widehat{\omega}_1$	$\widehat{\omega}_2$	$\widehat{\omega}_3$	$\widehat{\omega}_4$	$\widehat{\omega}_5$	$\widehat{\omega}_6$
FFFF	UD	1.7636	5.4514	6.3159	10.7226	13.8896	14.0269
	FG-X	1.8730	5.8528	6.7388	11.7280	15.3134	15.5988
FSFS	UD	2.3079	2.7308	8.2994	9.5016	12.4923	12.6919
	FG-X	2.4459	2.9059	8.9682	10.0600	12.5827	12.7878
CFFF	UD	2.3773	2.7899	6.0480	8.5095	11.2202	11.9149
	FG-X	2.8184	3.2002	6.5704	8.5693	12.2300	13.1720
CCFF	UD	2.4970	4.8398	10.9934	11.4707	11.9964	15.8960
	FG-X	2.9312	5.3033	11.5560	11.8834	13.2891	17.1274
FCFC	UD	4.8613	5.5816	12.4191	13.2226	17.2725	19.2883
	FG-X	5.1349	5.9713	13.3685	13.9516	19.1691	19.6810
SFSF	UD	6.3471	7.2211	10.6490	17.1753	20.4088	20.5056
	FG-X	7.3860	8.2251	11.6574	18.4773	20.6508	22.3821
SSSF	UD	6.6219	9.2224	10.2552	15.2407	20.5560	23.2678
	FG-X	7.6475	10.2068	10.3279	16.4122	22.5210	24.1566
SCSF	UD	6.7274	10.1301	10.2554	17.0292	20.6460	24.0183
	FG-X	7.7500	10.3281	11.1252	18.2793	22.6161	25.9162
SSSS	UD	7.9698	13.2784	20.5135	21.3031	22.2306	24.2303
	FG-X	8.9573	14.3516	20.6590	22.8072	24.1829	24.4337
SCSS	UD	9.1644	10.2555	16.0195	22.9656	24.1608	30.2926
	FG-X	10.1448	10.3282	17.1667	24.9225	25.8037	30.9830
SCSC	UD	9.5106	16.8645	20.5138	23.2036	24.9848	31.3500
	FG-X	10.4995	18.0591	20.6593	25.1488	26.6760	33.1816
CFCF	UD	10.9295	11.2611	13.4108	18.7423	23.7364	23.9021
	FG-X	11.8317	12.1688	14.3659	19.9358	24.2030	25.0527
CCCF	UD	11.0838	13.2095	18.7370	23.8167	26.3403	26.8482
	FG-X	11.9890	14.1549	19.9079	25.1517	27.7913	28.2863
CCCC	UD	12.9865	18.7299	26.2869	26.3612	33.0683	33.9720
	FG-X	13.9237	19.8764	27.6600	27.8182	34.6762	35.6684

homogeneous material where skew angle is $\alpha = 30^\circ$. Only flexural modes are considered in the analysis of Liew et al. [44] and for the sake of comparison, the same is done is the present research by dropping out the in-plane displacement components. Results are compared with the results of Liew et al. [44] which are also obtained according to the first order shear deformation plate theory. Various cases of boundary conditions are considered for the edges of the plate. As seen results are in excellent agreement with the available data in the open literature.

The next comparison study is devoted to first six frequencies of composite laminated skew plates. It is known that, in cross-ply lamination scheme, the stiffness components $A_{16}, A_{26}, B_{16}, B_{26}$, D_{16} and D_{26} are absent and therefore presented formulation also may be used for frequency analysis of cross-ply composite skew plates. Three different skew angles are taken into consideration and stacking sequence is [90/0/90/0/90]. Since the stacking sequence is symmetric, in-plane and out-of-plane vibrations are separate. For the sake of comparison only flexural frequencies are evaluated. Plates are assumed to be thin for the sake of comparison. The aspect ratio is $a/b = 1$. Results of our study are compared with those of Wang [45]. Comparison is carried out in Table 4. It is observed that, our results are in excellent agreement with those of Wang [45] which guarantees the accuracy and efficiency of the proposed method.

6.2. Parametric studies

After validating the proposed formulation and solution method, parametric studies are given in this section to study the natural frequencies of FG-CNTRC skew plates with various boundary conditions. In whole of this section frequency parameter is defined as $\widehat{\omega} = \omega b^2\sqrt{\rho_m h/D_m}/\pi^2$.

Table 5 presents the first six frequency parameters of FG-CNTRC skew plates where geometrical characteristics of the plate are $a/b = 1$ and $b/h = 20$. In this table, three different volume fractions of CNTs, three different skew angles and four different cases of CNT dispersion profiles are considered. Numerical results of this table are provided for a plate which is clamped all around. As seen from the tabulated results in this table, enrichment of the polymeric matrix with more carbon nanotube results in higher frequencies of the plate. Therefore, plates with higher CNT volume fraction have higher frequencies. Among the four cases of CNT dispersion pattern across the plate thickness, FG-X pattern results in higher frequencies and FG-O pattern results in lower frequencies. It is also should be mentioned that, in FG-X, FG-O and UD types, flexural modes are independent from the in-plane modes since the properties of the plate are graded symmetrically with respect to the plate mid-surface. In such conditions, the extensional-bending couplings are absent. On the other hand, for FG-V skew plates where distribution of CNT across the plate is not symmetric, flexural and in-plane vibrations are coupled and therefore for accurate vibration analysis, in-plane displacement components and out-of-plane displacement components should be taken into account together. It is observed that with increasing the skew angle of the plate, frequencies also increase. This is due to the fact that, plate area decreases as the defined skew angle increases. Because of the reduction in area, the stiffness of the plate increases, leading to the frequency enhancement.

Table 7
First six natural frequency parameters $\widehat{\omega} = \omega b^2 \sqrt{\rho_m h / D_m}/\pi^2$ for skew plates with CCCC boundary conditions and various side to thickness ratios. Characteristics of the plate are $a/b = 1$ and $V^*_{CN} = 0.17$.

α	b/h	Type	$\widehat{\omega}_1$	$\widehat{\omega}_2$	$\widehat{\omega}_3$	$\widehat{\omega}_4$	$\widehat{\omega}_5$	$\widehat{\omega}_6$
0°	100	UD	15.6206	17.6535	22.6646	31.1104	41.0435	42.1920
		FG-X	18.7294	20.6357	25.5149	34.0312	46.0554	48.8590
	20	UD	10.7650	13.0862	18.2481	22.3434	23.7065	25.9533
		FG-X	11.6378	14.0031	19.3343	23.5866	24.9799	27.3335
	10	UD	6.8629	9.4126	12.9177	14.0013	14.5263	16.0096
		FG-X	7.1091	9.7837	13.2948	14.5490	14.9830	16.1604
15°	100	UD	15.7352	18.0683	23.6095	32.6953	41.2120	42.5879
		FG-X	18.8356	21.0372	26.4740	35.7079	48.4204	49.0133
	20	UD	10.8919	13.4983	19.0238	22.5429	24.2298	26.5307
		FG-X	11.7672	14.4291	20.1444	23.7925	25.5218	27.9408
	10	UD	7.0041	9.7708	13.1393	14.2270	15.3449	16.6085
		FG-X	7.2574	10.1556	13.5259	14.7403	15.8679	16.7653
30°	100	UD	16.2142	19.6857	27.0574	38.1048	41.9546	44.3336
		FG-X	19.2847	22.6293	30.0368	41.5850	49.6886	51.8767
	20	UD	11.4123	15.0207	21.5717	23.4079	26.4269	28.8189
		FG-X	12.3012	16.0088	22.8119	24.6875	27.7964	30.3308
	10	UD	7.5543	10.9862	14.0701	15.2874	17.8404	18.5976
		FG-X	7.8338	11.4117	14.4951	15.8070	18.4475	18.7740
45°	100	UD	17.7656	24.1464	35.2777	44.3183	49.2694	50.1981
		FG-X	20.7785	27.1752	38.8685	51.7803	54.4633	57.4944
	20	UD	12.9865	18.7299	26.2869	26.3612	33.0683	33.9720
		FG-X	13.9237	19.8764	27.6600	27.8182	34.6762	35.6684
	10	UD	9.0390	13.4607	16.9083	17.7452	21.9874	22.6272
		FG-X	9.3782	13.9444	17.4347	18.2980	22.5835	23.0152
60°	100	UD	23.7514	36.8564	53.0979	55.8751	71.3202	73.7827
		FG-X	26.7982	40.8002	59.0269	63.0920	79.3177	81.1861
	20	UD	18.3160	27.2434	35.8500	37.4982	44.6560	49.4709
		FG-X	19.4256	28.7330	37.6159	39.2064	46.5953	51.5734
	10	UD	13.2309	18.5795	23.1690	25.2704	27.6134	31.5316
		FG-X	13.6857	19.1497	23.7768	25.9851	28.2393	32.2393

Since among the three different functionally graded patterns of CNT volume fraction, FG-X pattern results in higher frequencies, in the subsequent results only FG-X type is considered.

A comparison on the effect of boundary conditions of the plate on the natural frequencies of the FG-CNTRC plates is presented in Table 6. Plates with aspect ratio $a/b = 1$, side to thickness ratio $b/h = 20$ and CNT volume fraction $V^*_{CN} = 0.17$ are considered. Various combinations of free, simply supported and clamped edges are considered. As expected, plates with all edges free have the lowest frequencies and those which are clamped all around have the highest frequencies. It is seen that, when one edge of the plate changes form free to simply supported or from simply supported to clamped, frequencies of the plate enhance. This trend is due to the increase in the local flexural rigidity of the plate with stiffening the edge support. Similar to the conclusion of the previous table, for all of the studied cases, FG-X pattern results in higher frequencies in comparison to UD pattern when all of the other geometrical characteristics are kept constant. This is due to the higher flexural stiffness of an FG-X pattern in comparison to UD pattern.

The effect of thickness is investigated in the next table. Table 7 provides the first six frequencies of skew plates which are clamped all around. Five skew angles are considered and both UD and FG-X plates are considered. In each case, a thin ($a/h = 100$), a moderately thick ($a/h = 20$) and a thick ($a/h = 10$) plate are considered. Results confirm the fact that frequencies of FG-X plate are higher than those of UD plate. Increasing the skew angle of the plate results in higher frequencies which is expected. Furthermore, the influence of thickness is observant since the non-dimensional frequency parameter varies essentially with respect to thickness ratio.

Fig. 2 depicts the variation of first three frequencies of skew plates with respect to skew angle. Aspect ratio $a/b = 1$, side to thickness ratio $a/h = 20$ and CNT volume fraction $V^*_{CN} = 0.12$ are pre-assumed. Distribution of CNT across the plate thickness is assumed to be uniform. It is seen that for all of the studied cases of boundary conditions, which are CCCF, CFCF, SCSC, SCSS, SFSF and SSSS, increasing the skew angle enhances the frequencies of the plate.

Fig. 3 aims to investigate the influence of aspect ratio on the first three frequencies of FG-CNTRC plates with various combinations of boundary conditions. In this figure, CNTs are distributed according to the FG-X pattern across the thickness. Furthermore, geometrical characteristics are $\alpha = 45°$, $a/h = 20$, $V^*_{CN} = 0.12$. Obviously, when b and h are constant, with increasing a, frequencies of the plate decrease. This trend happens almost for all of the boundary conditions.

7. Conclusion

Free vibration response of carbon nanotube reinforced composite plates in a skew shape is investigated in the present research. Distribution of reinforcement through the thickness of the matrix may be uniform or functionally graded. Properties of the composite media are estimated according to a modified rule of mixtures approach with introduction of efficiency parameters. The components of displacement field are transformed from an orthogonal coordinate system to an oblique one. The total strain and kinetic energies of the skew plate are obtained. The conventional Ritz formulation is used to deduce the matrix representation of the equations of motion associated to the free vibration motion. Shape functions are estimated according to the orthogonal polynomials developed according to the Gram–Schmidt process. The resulting eigenvalue problem is established. Comparison and convergence studies are carried out to assure the correctness and efficiency of the proposed method. Afterwards parametric studies are given to obtain the frequencies of carbon nanotube reinforced skew plates. It is shown that, increasing the volume fraction of carbon nan-

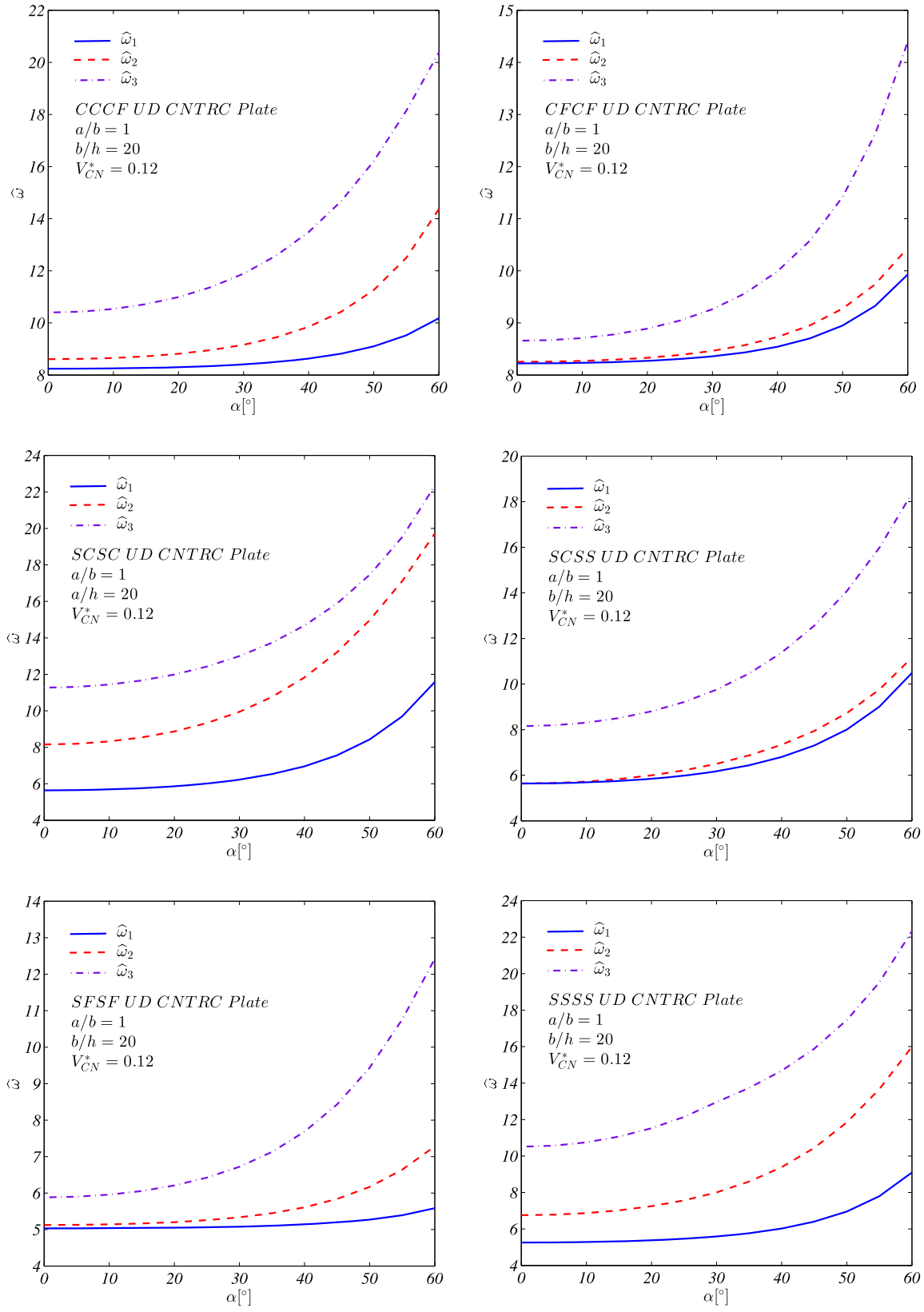

Fig. 2. Variation of first three frequencies of UD-CNTRC skew plates with respect to skew angle for plates with $a/b = 1$, $b/h = 20$, $V^*_{CN} = 0.12$ and various types of boundary conditions.

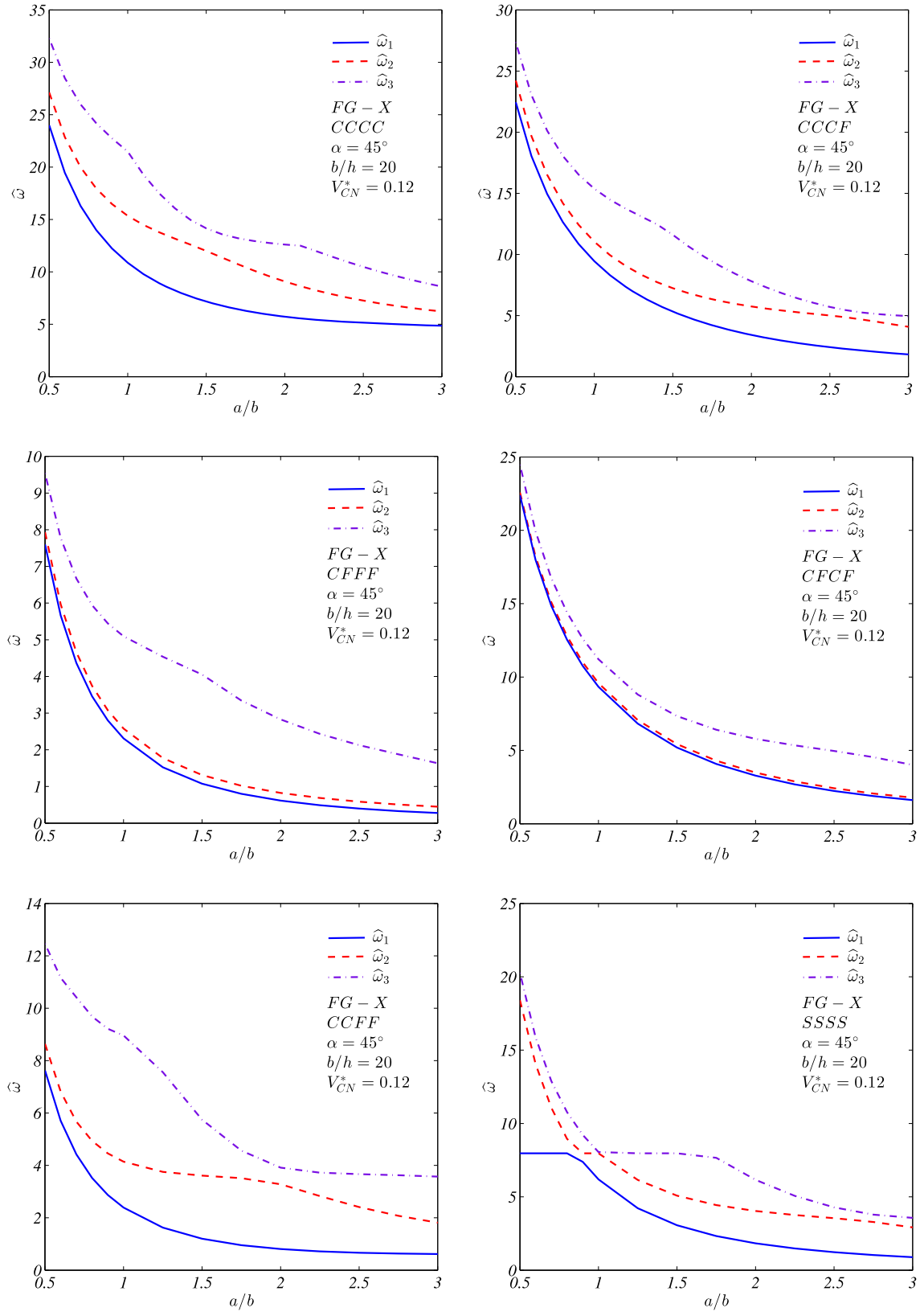

Fig. 3. Variation of first three frequencies of FG-X CNTRC skew plates with respect to aspect ratio for plates with $\alpha = 45°$, $b/h = 20$, $V^*_{CN} = 0.12$ and various types of boundary conditions.

otubes increases the frequencies of the plate. Furthermore, through a proper functionally graded distribution of carbon nanotubes, frequencies of the plate may be controlled. In all of the cases, FG-X pattern has higher frequencies in comparison to UD pattern and UD pattern has higher frequencies in comparison to FG-O pattern. Similar to isotropic homogeneous, composite laminated and functionally graded skew plates, increasing the skew angle enhances the frequencies of the plate when of the all other geometrical and material properties are kept constant.

Conflict of interest statement

There is no conflict of interest.

References

[1] K.M. Liew, Z.X. Lei, L.W. Zhang, Mechanical analysis of functionally graded carbon nanotube reinforced composites: a review, Compos. Struct. 120 (2015) 90–97.

[2] H.S. Shen, Nonlinear bending of functionally graded carbon nanotube reinforced composite plates in thermal environments, Compos. Struct. 91 (2009) 9–19.

[3] P. Zhu, Z.X. Lei, K.M. Liew, Static and free vibration analyses of carbon nanotube-reinforced composite plates using finite element method with first order shear deformation plate theory, Compos. Struct. 94 (2012) 1450–1460.

[4] L.W. Zhang, Z.X. Lei, K.M. Liew, Vibration characteristic of moderately thick functionally graded carbon nanotube reinforced composite skew plates, Compos. Struct. 122 (2015) 172–183.

[5] L.W. Zhang, Z.X. Lei, K.M. Liew, Free vibration analysis of functionally graded carbon nanotube-reinforced composite triangular plates using the FSDT and element-free IMLS-Ritz method, Compos. Struct. 120 (2015) 189–199.

[6] L.W. Zhang, Z.G. Song, K.M. Liew, State-space Levy method for vibration analysis of FG-CNT composite plates subjected to in-plane loads based on higher-order shear deformation theory, Compos. Struct. 134 (2015) 989–1003.

[7] L.W. Zhang, W.C. Cui, K.M. Liew, Vibration analysis of functionally graded carbon nanotube reinforced composite thick plates with elastically restrained edges, Int. J. Mech. Sci. 103 (2015) 9–21.

[8] L.W. Zhang, Z.X. Lei, K.M. Liew, Computation of vibration solution for functionally graded carbon nanotube-reinforced composite thick plates resting on elastic foundations using the element-free IMLS-Ritz method, Appl. Math. Comput. 256 (2015) 488–504.

[9] Z.X. Lei, L.W. Zhang, K.M. Liew, Free vibration analysis of laminated FG-CNT reinforced composite rectangular plates using the kp-Ritz method, Compos. Struct. 127 (2015) 245–259.

[10] P. Malekzadeh, A.R. Zarei, Free vibration of quadrilateral laminated plates with carbon nanotube reinforced composite layers, Thin-Walled Struct. 82 (2014) 221–232.

[11] P. Malekzadeh, Y. Heydarpour, Mixed Navier-layerwise differential quadrature three-dimensional static and free vibration analysis of functionally graded carbon nanotube reinforced composite laminated plates, Meccanica 50 (2015) 143–167.

[12] S. Natarajan, M. Haboussi, G. Manickam, Application of higher-order structural theory to bending and free vibration analysis of sandwich plates with CNT reinforced composite facesheets, Compos. Struct. 113 (2014) 197–207.

[13] Z.X. Wang, H.S. Shen, Nonlinear vibration of nanotube-reinforced composite plates in thermal environments, Comput. Mater. Sci. 50 (2011) 2319–2330.

[14] Z.X. Wang, H.S. Shen, Nonlinear vibration and bending of sandwich plates with nanotube-reinforced composite face sheets, Composites, Part B, Eng. 43 (2012) 411–421.

[15] M. Mirzaei, Y. Kiani, Free vibration of functionally graded carbon nanotube reinforced composite plates with cut-out, Beilstein J. Nanotechnol. 7 (2016) 511–523.

[16] M. Wang, Z.M. Li, P. Qiao, Semi-analytical solutions to buckling and free vibration analysis of carbon nanotube-reinforced composite thin plates, Compos. Struct. 144 (2016) 33–43.

[17] Y. Kiani, Free vibration of carbon nanotube reinforced composite plate on point Supports using Lagrangian multipliers, Meccanica (2016), http://dx.doi.org/10.1007/s11012-016-0466-3.

[18] E. Garcia-Macias, R. Castro-Triguero, E.I.S. Flores, M.I. Friswell, R. Gallego, Static and free vibration analysis of functionally graded carbon nanotube reinforced skew plates, Compos. Struct. 140 (2016) 473–590.

[19] Z.X. Lei, L.W. Zhang, K.M. Liew, Elastodynamic analysis of carbon nanotube reinforced functionally graded plates, Int. J. Mech. Sci. 99 (2015) 208–217.

[20] Z.X. Wang, H.S. Shen, Nonlinear dynamic response of nanotube-reinforced composite plates resting on elastic foundations in thermal environments, Nonlinear Dyn. 70 (2012) 735–754.

[21] P. Malekzadeh, M. Dehbozorgi, S.M. Monajjemzadeh, Vibration of functionally graded carbon nanotube-reinforced composite plates under a moving load, Sci. Eng. Compos. Mater. 22 (2015) 37–55.

[22] H. Kwon, C.R. Bradbury, M. Leparoux, Fabrication of functionally graded carbon nanotube-reinforced aluminum matrix composite, Adv. Eng. Mater. 13 (2013) 325–329.

[23] H.S. Shen, Postbuckling of nanotube-reinforced composite cylindrical shells in thermal environments, part I: axially-loaded shells, Compos. Struct. 93 (2011) 2096–2108.

[24] J.E. Jam, Y. Kiani, Buckling of pressurized functionally graded carbon nanotube reinforced conical shells, Compos. Struct. 125 (2015) 586–595.

[25] M. Mirzaei, Y. Kiani, Thermal buckling of temperature dependent FG-CNT reinforced composite conical shells, Aerosp. Sci. Technol. 47 (2015) 42–53.

[26] D.L. Shi, X.Q. Feng, Y.Y. Huang, K.C. Hwang, H.J. Gao, The effect of nanotube waviness and agglomeration on the elastic property of carbon nanotube reinforced composites, J. Eng. Mater. Technol. 126 (2004) 250–257.

[27] J.D. Fidelus, E. Wiesel, F.H. Gojny, K. Schulte, H.D. Wagner, Thermo-mechanical properties of randomly oriented carbon/epoxy nanocomposites, Composites, Part A, Appl. Sci. Manuf. 36 (2005) 1555–1561.

[28] S.H. Tagrara, A. Benachour, M.B. Bouiadjra, A. Tounsi, On bending, buckling and vibration responses of functionally graded carbon nanotube-reinforced composite beams, Steel Compos. Struct. 19 (2015) 1259–1277.

[29] J.E. Jam, Y. Kiani, Low velocity impact response of functionally graded carbon nanotube reinforced composite beams in thermal environment, Compos. Struct. 132 (2015) 35–43.

[30] M. Mirzaei, Y. Kiani, Snap-through phenomenon in a thermally postbuckled temperature dependent sandwich beam with FG-CNTRC face sheets, Compos. Struct. 134 (2015) 1004–1013.

[31] M. Mirzaei, Y. Kiani, Nonlinear free vibration of temperature dependent sandwich beams with carbon nanotube reinforced face sheets, Acta Mech. 227 (2016) 1869–1884.

[32] Y. Kiani, Thermal postbuckling of temperature-dependent sandwich beams with carbon nanotube-reinforced face sheets, J. Therm. Stresses 39 (2016) 1098–1110.

[33] S.J. Salami, Dynamic extended high order sandwich panel theory for transient response of sandwich beams with carbon nanotube reinforced face sheets, Aerosp. Sci. Technol. 56 (2016) 56–69.

[34] M. Mirzaei, Y. Kiani, Thermal buckling of temperature dependent FG-CNT reinforced composite plates, Meccanica 51 (2016) 2185–2201.

[35] M. Mirzaei, Y. Kiani, Free vibration of functionally graded carbon nanotube reinforced composite cylindrical panels, Compos. Struct. 142 (2016) 45–56.

[36] Y. Kiani, Torsional vibration of functionally graded carbon nanotube reinforced conical shells, Sci. Eng. Compos. Mater. (2016), http://dx.doi.org/10.1515/secm-2015-0454.

[37] M. Bennoun, M.S.A. Houaria, A. Tounsi, A novel five-variable refined plate theory for vibration analysis of functionally graded sandwich plates, Mech. Adv. Mat. Struct. 23 (2016) 423–431.

[38] Z. Belabed, M.S.A. Houari, A. Tounsi, S.R. Mahmoud, O.A. Beg, An efficient and simple higher order shear and normal deformation theory for functionally graded material (FGM) plates, Composites, Part B, Eng. 60 (2014) 274–283.

[39] H. Hebali, A. Tounsi, M. Houari, A. Bessaim, E. Bedia, A new quasi-3D hyperbolic shear deformation theory for the static and free vibration analysis of functionally graded plates, J. Eng. Mech. 140 (2014) 374–383.

[40] J.N. Reddy, Mechanics of Laminated Composite Plates and Shells, Theory and Application, CRC Press, Boca Raton, 2003.

[41] H.S. Shen, Y. Xiang, Nonlinear analysis of nanotube-reinforced composite beams resting on elastic foundations in thermal environments, Eng. Struct. 56 (2013) 698–708.

[42] Y. Han, J. Elliott, Molecular dynamics simulations of the elastic properties of polymer/carbon nanotube composites, Comput. Mater. Sci. 39 (2007) 315–323.

[43] C.Y. Wang, L.C. Zhang, A critical assessment of the elastic properties and effective wall thickness of single-walled carbon nanotubes, Nanotechnology 19 (2008) 075705.

[44] K.M. Liew, Y. Xiang, S. Kitipornchai, C.M. Wang, Vibration of thick skew plates based on Mindlin shear deformation plate theory, J. Sound Vib. 168 (1993) 39–69.

[45] S. Wang, Vibration of thin skew fibre reinforced composite laminates, J. Sound Vib. 201 (1997) 335–352.